

Changes of interlayer exchange coupling in Fe/Si/Fe trilayer structure by photo-irradiation

S. Ueda,^{1,2,*} Y. Iwasaki,^{1,3,*} Y. Uehara,^{1,4,*} and S. Ushioda^{1,5,*}

¹RIKEN Photodynamics Research Center, Aoba-ku, Sendai 980-0845, Japan

²NIMS Beamline Station at SPring-8, National Institute for Materials Science, Sayo, Hyogo 678-5148, Japan

³Core Component Business Group, Sony Corporation, Tagajo, Miyagi 985-0842, Japan

⁴Research Institute of Electrical Communication, Tohoku University, Aoba-ku, Sendai 980-8577, Japan

⁵National Institute for Materials Science, Sengen, Tsukuba 305-0047, Japan

(Received 18 September 2010; revised manuscript received 6 February 2011; published 25 April 2011)

The interlayer exchange coupling of the room-temperature-grown Fe/Si/Fe trilayer structure was studied by using spin-polarized secondary-electron microscopy. For the nominal Si spacer thickness in the 0.5–5.0 nm range, the interlayer exchange coupling between the Fe layers measured at room temperature was always ferromagnetic, and had a maximum at the nominal Si spacer thickness of 1.3 nm. By the laser irradiation ($\lambda = 532$ nm and the intensity of 28.4 mW/mm²), the interlayer exchange coupling weakened at the spacer thickness below 2.7 nm, while the ferromagnetic coupling between the Fe layers still remained. These phenomena can be qualitatively understood by the assisted tunneling theory with spin-flip processes in the semiconducting spacer layer.

DOI: 10.1103/PhysRevB.83.144424

PACS number(s): 75.70.-i, 78.20.Ls, 68.37.Hk

I. INTRODUCTION

The research fields of spintronics have opened the horizon of device applications utilizing the spin degree of freedom. Since the discovery of oscillatory interlayer exchange coupling¹ and giant magnetoresistance (GMR)² in multilayer structures with ferromagnetic metals (FM) separated by nonmagnetic materials, a wide variety of artificial multilayer structures has been intensively studied.^{3–7} At the first stage of research on artificial multilayer structures, FM separated by nonmagnetic metals (NM) has been studied to explore the GMR effects and the behavior of interlayer exchange interaction as a function of the thickness of NM layers. Then semiconductors (S) and insulators were used as a spacer layer between FM layers.^{8–15} For the [FM/S]_n multilayer structures (*n* is the number of periods), the strong temperature dependence of interlayer exchange coupling and magnetization reversal behavior were reported.^{9,14,15}

[FM/S]_n multilayer structures also show an interlayer exchange coupling as well as a NM spacer layer. For multilayer structures with a S spacer layer, the strength of interlayer exchange coupling depends on temperature.⁹ The sign and strength of the interlayer exchange coupling depend on the condition of sample preparation.⁸ In addition, Mattson *et al.*¹⁰ reported that the sign of interlayer exchange coupling was modified by photo-irradiation at low temperature. The transition from ferromagnetic to antiferromagnetic interlayer exchange coupling by photo-irradiation was reported in Ref. 10. For the Fe/Si/Fe trilayer structure at room temperature (RT), however, a detailed experimental report has not yet been done on the dependence of interlayer exchange coupling on the Si spacer thickness. For this system at RT, only Briner and Landolt⁹ reported that the alternative change of the sign in the interlayer exchange coupling was not observed.

To clarify the detailed behavior of the interlayer exchange coupling as a function of Si spacer thickness under dark and photo-irradiation conditions at RT, we have studied the Fe/Si/Fe trilayer structure using spin-polarized secondary-electron microscopy (SP-SEM). A nonmagnetic probe of SP-SEM with a yoke of an electromagnet and a visible

light laser enables us to determine the changes of interlayer exchange coupling on Si spacer thickness under dark and light conditions. To determine the interlayer exchange coupling, the trilayer structure is useful because the interlayer exchange coupling between two ferromagnetic layers is simply given as follows:

$$J_{\text{ex}} = tMH_{\text{ex}}, \quad (1)$$

where J_{ex} , t , M , and H_{ex} are the interlayer exchange coupling, the thickness of the top magnetic layer, magnetization, and exchange bias field, respectively. In this work, we report on the interlayer exchange coupling strength of the Fe/Si/Fe trilayer structure at RT as a function of the Si spacer thickness under dark and light conditions.

II. EXPERIMENT

The SP-SEM system^{16,17} has a field-emission gun (FE-1000, EIKO engineering) and a medium-energy (25 kV) Mott spin detector of retarding potential type. The primary electron beam with 15 keV was incident at 45° from the surface normal. The Mott spin detector measures two in-plane components of polarization P_x and P_y , simultaneously, which allows us to determine the direction of the magnetization vector in the film plane. The spatial resolution of our SP-SEM was 100 nm. A solenoid-coil electromagnet in the SP-SEM chamber¹⁶ was replaced by a yoke of an electromagnet in the present SP-SEM system.¹⁷ To apply a magnetic field to the sample, the yoke of an electromagnet was used in this work. Magnetic imaging of the sample in remanent states after application of a magnetic field was performed under ultrahigh vacuum (UHV) better than 4.0×10^{-10} Torr at RT. The continuous wave second-harmonic-generated light of an Nd-YAG laser ($\lambda = 532$ nm) was irradiated onto the sample from a viewing port of the SP-SEM system.

The Fe/Si/Fe trilayer structure was prepared *in situ* by an e-beam deposition on a Cr (3 nm)/ native oxidized Si substrate at RT. First, we deposited polycrystalline layers of 3-nm-thick Cr and 10-nm-thick Fe on the native oxidized Si substrate in this sequence by using e-beam evaporators

(EFM-3T, OMICRON) in the preparation chamber attached to the SP-SEM. After the deposition, we checked the coercivity (H_C) of the Fe layer by the SP-SEM. H_C of the Fe layer was found to be 23.2 Oe. Then we applied a magnetic field of 59 Oe to prepare the single magnetic domain state. After applying the magnetic field, we deposited the amorphous Si spacer layer by using the e-beam evaporators with a nominal thickness range of 0.5–6.0 nm on the Fe(10 nm)/Cr(3 nm)/Si substrate through a moving slit. Finally a 3-nm-thick Fe layer was deposited on the Si(0.5–6.0 nm)/Fe(10 nm)/Cr(3 nm)/Si substrate. Deposition rates of Fe, Cr, and Si were about 0.05 nm/min and were calibrated by a quartz-oscillator film-thickness gauge. The pressure of the preparation chamber was better than 4.0×10^{-10} Torr during the evaporation.

III. RESULTS AND DISCUSSION

Figure 1 shows the magnetic images of the Fe/Si/Fe trilayer structure in remanent states after applying a magnetic field. The field of view of each image is $100 \mu\text{m}$ (y axis) \times $2100 \mu\text{m}$ (x axis). The magnetic images in Fig. 1 display the magnetization of the top Fe layer due to a probing depth of ~ 1 nm in the SP-SEM measurements. The magnetization direction and spin polarization (P_y) are illustrated by dark ($-y$ direction) and bright ($+y$ direction) contrast. The P_x component is negligibly weak in all the magnetic images. The magnetic domain structure of Fe/Si/Fe was not affected by a magnetic field applied to the $-y$ direction up to 15.7 Oe. We note that the as-made magnetic domain structure was the same as the top magnetic image in Fig. 1. Furthermore, the magnetization direction was oriented to the $+y$ direction for the entire Si spacer thickness. This suggests that the interlayer exchange coupling between the top and bottom Fe layers is always ferromagnetic for the entire Si spacer thickness, while P_y was decreased around the Si spacer thickness of 1.5 nm. We note that P_x was negligibly weak in this experiment. The decrease of P_y around the Si spacer thickness of 1.5 nm may be due to the noncollinear coupling between the top and bottom Fe layers, or the net exchange interaction of ferromagnetic coupling in which the ferromagnetic and antiferromagnetic coupled states are mixed.^{18,19} In the spatial resolution of our SP-SEM, the magnetic domain separation due to the above-mentioned mechanism was not found. The magnetization reversal of the top Fe layer occurred around the Si spacer thickness in the range between 2.9 and 5.0 nm after applying the magnetic field of 17.4 Oe. The reversed magnetization area expands with increasing magnetic field. In the thin Si spacer region (0.5–1.5 nm), the magnetization reversal started at the applied field of 25.7 Oe. The magnetization for the entire Si spacer thickness was completely reversed by applying the magnetic field of 29.0 Oe. These results clearly show that the reversal magnetic field for the Fe/Si/Fe trilayer structure depends on the Si spacer thickness. In addition, the behavior of J for the RT grown Fe/Si/Fe trilayer structure is different from that for the low-temperature (LT) grown one. For the LT grown Fe/Si/Fe trilayer structure, the oscillation of the interlayer exchange coupling at LT has been reported in Refs. 8 and 9. In the RT grown Fe/Si/Fe trilayer structure, the intermixing at the interface between the Fe and Si layers has been reported, but

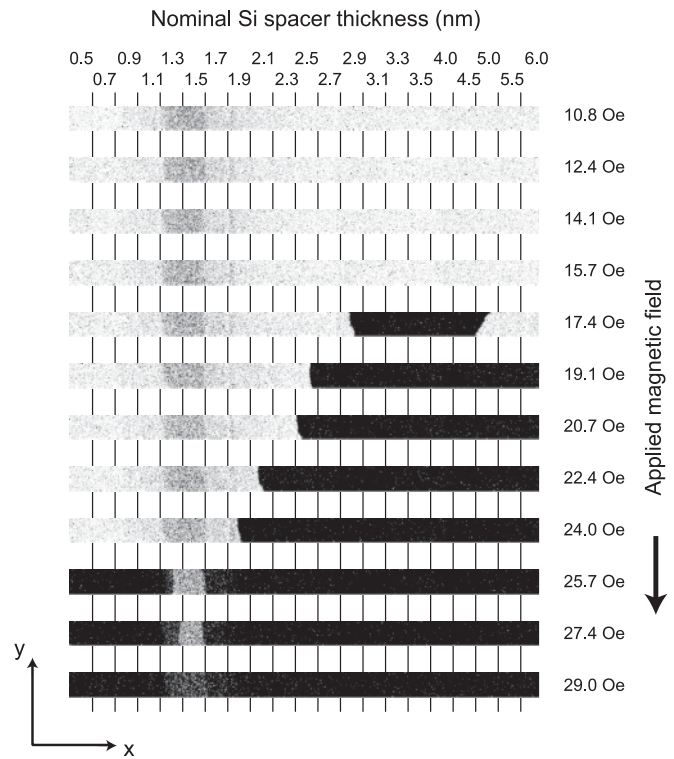


FIG. 1. Magnetization reversal process of the Fe/Si/Fe trilayer structure in the dark condition. The magnetic images were measured in remanent states. Bright contrast corresponds to magnetization along the $+y$ direction, and dark contrast corresponds to that along the $-y$ direction. In the magnetization reversal measurements, magnetic field was applied along the $-y$ direction.

first we neglect the intermixing effect to discuss the interlayer exchange coupling of the RT grown Fe/Si/Fe trilayer structure for simplicity.

Figure 2 shows the magnetic images of the Fe/Si/Fe trilayer structure in remanent states after applying a magnetic field under photo-irradiation ($\lambda = 532$ nm, 28.4 mW/mm²). The field of view of each image is $100 \mu\text{m}$ (y axis) \times $1600 \mu\text{m}$ (x axis). By the photo-irradiation, the magnetization reversal behavior seen in Fig. 2 was modified in comparison with that seen in Fig. 1. In the thin Si spacer region (< 3 nm) under the photo-irradiation condition, one can see that the magnetization reversal occurred by a slightly lower magnetic field than that measured in the dark (non-photo-irradiation) condition. We obtained the magnetization reversal fields for the entire Si spacer thickness, and deduced the strength of interlayer exchange coupling (J) for both the dark and photo-irradiation conditions.

Figure 3 shows the distribution of J as a function of the Si spacer thickness. Here we employed H_{ex} in Eq. (1) as the H_C difference between the top and bottom Fe layers. H_C of the top Fe layers was obtained from SP-SEM images. The magnitude of J in the dark condition varied from 0.4 to $5.8 \mu\text{J}/\text{m}^2$, as seen in Fig. 3. The magnitude of J is the same order in comparison with other FM/S/FM trilayer structures as reported in Refs. 9 and 15. This result suggests that the intermixing of Fe and Si is not significant, especially in the inside Si barrier layer. If the intermixing is significant in the Si layer inside, Fe silicides will

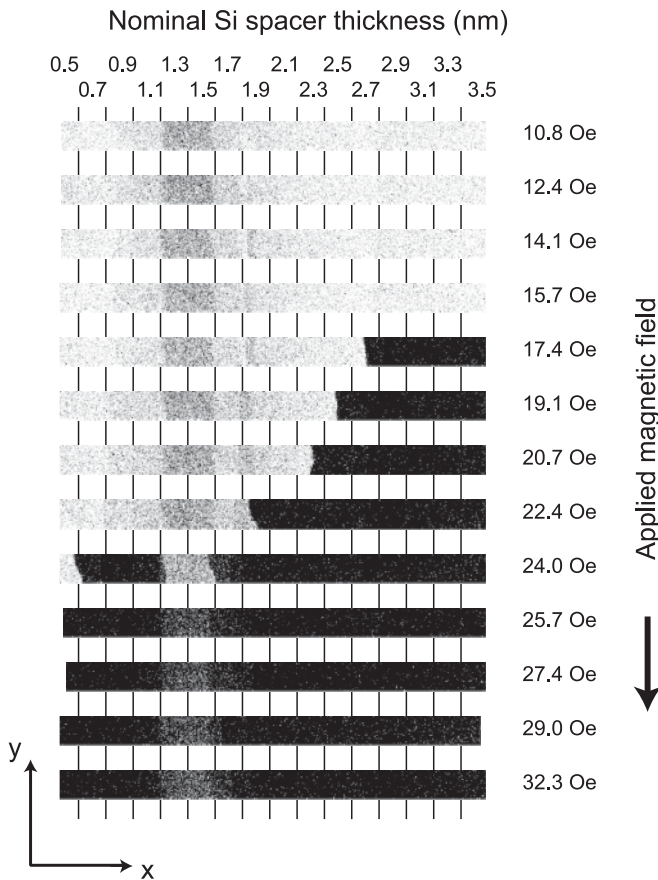


FIG. 2. Magnetization reversal process of the Fe/Si/Fe trilayer structure in the photo-irradiation condition ($\lambda = 532$ nm, 28.4 mW/mm²). The magnetic images were measured in remanent states.

be formed and the interlayer exchange coupling strength will be enhanced. In fact, the coupling strength of the Fe/FeSi/Fe trilayer structure^{20,21} grown by a molecular-beam epitaxial method is two orders of magnitude stronger than that of our sample. In addition, the Fe/FeSi/Fe trilayer structure clearly showed the antiferromagnetic interlayer exchange coupling at RT. Furthermore, the changes of spin polarization of secondary electrons from the top Fe layer in our sample, except for the thin Si spacer around 1.3 nm thickness, were not observed in comparison with the polycrystalline bottom Fe layer. The constant reversal field seen in the thin Si spacer below 1.1 nm may be due to the presence of pinholes in the spacer layer. We could not deny the intermixing between the Fe and Si layers as reported in Refs. 20 and 22, but we considered that the intermixing was a minor role in the exchange coupling behavior on the Si spacer thickness. In the dark condition, J showed the maximum at the Si spacer thickness of 1.3 nm. J steeply decreased with increasing Si spacer thickness above 1.5 nm, while J was almost constant in the thin Si spacer region below 1.1 nm. The behavior of J was similar in both the dark and photo-irradiation conditions. The magnitude of J in the photo-irradiation condition varied from 0.4 to 4.4 $\mu\text{J}/\text{m}^2$, as seen in Fig. 3. The obvious difference in the magnitude of J was found in the 0.5–2.7-nm-thick Si spacer region even at RT; J for the photo-irradiation condition was smaller than that

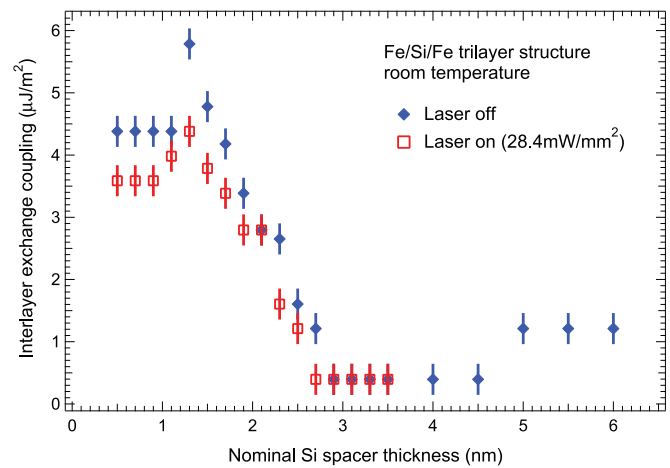


FIG. 3. (Color online) Interlayer exchange-coupling dependence of the nominal Si spacer thickness in the dark and photo-irradiation conditions.

for the dark condition for the Si spacer thickness between 0.5 and 2.7 nm. We considered that this difference originated from a photo-irradiation effect.

To clarify the photo-irradiation effect in detail, we measured the irradiation laser power dependence on the magnetization reversal of the Fe/Si/Fe trilayer structure. Figure 4 shows the magnetic images of the Fe/Si/Fe trilayer structure with the Si spacer thickness between 0.9 and 1.9 nm under the photo-irradiation condition at the laser power of 12.3, 20.5, and 28.4 mW/mm². Before measuring the magnetic images in remanent states, the magnetic field of 59.0 Oe along the +y direction was applied to the sample to obtain the single magnetic domain, and then the magnetic field of 24.0 Oe along the -y direction was applied to observe the magnetization reversal under the photo-irradiation condition. As seen in Fig. 4, obvious magnetization reversal in the Si spacer thickness of 0.9 and 1.1 nm was observed at the laser power of 20.5 and 28.4 mW/mm², while the magnetization reversal did not occur at that of 12.3 mW/mm². We note that an increase in the sample temperature (ΔT) by 28.4 mW/mm² laser irradiation was about 9 K, which was checked *ex situ* by using an alumel-chromel thermocouple. In addition, we also measured an increase in temperature when we placed

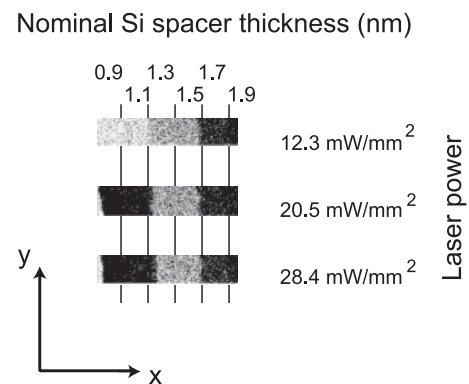


FIG. 4. Irradiated laser power dependence of magnetization reversal for the Fe/Si/Fe trilayer structure with the nominal Si spacer thickness in the 0.9–1.9 nm range.

the thermocouple in the laser beam with 28.4 mW/mm^2 . This temperature increase was in agreement with ΔT . ΔT is about 3 K by increasing the laser power shown in Fig. 4. If ΔT plays a major role in weakening J , the magnetization reversal should be drastically changed between the 20.5 and 28.4 mW/mm^2 photo-irradiation conditions. But such a change was not observed in this work. Thus, a thermal effect may play a minor role in weakening J by the photo-irradiation, as seen in Fig. 3. We expected that a photo-irradiation effect played an important role in weakening J . Since we irradiated the laser with $\lambda = 532 \text{ nm}$, which was shorter than the band-gap energy of Si, to the Fe/Si/Fe trilayer structure, it was considered that photoexcited carriers created in the Si spacer layer affected the interlayer exchange coupling between the top and bottom Fe layers.

There are many theoretical works to interpret the interlayer exchange coupling on trilayer structures. The Ruderman-Kittel-Kasuya-Yosida (RKKY) -based theory²³ reproduces well the behavior of the interlayer exchange coupling for the trilayer structures with NM spacer layers. However, the theory is not suitable for treating FM/S/FM trilayer structures, because the Fermi wave vector (k_F) is sufficiently small in semiconductors. The extended RKKY interaction theory has been reported by Shi and Klein²⁴ for a narrow-gap semiconductor, but the band-gap energy of amorphous Si is too large to treat appropriately as described in their work. Thus these theories are not suitable to explain the behavior of interlayer exchange coupling of the Fe/Si/Fe structure in both the dark and photo-irradiation conditions.

It is known that amorphous Si consists of defect states.²⁵ The defect states in the Si spacer layer can affect the interlayer exchange coupling in the Fe/Si/Fe structure. Furthermore, by the photo-irradiation to the Fe/Si/Fe structure, photoexcited carriers can be created in the Si spacer, and can be trapped in the defect states. Therefore, we expect that the assisted tunneling process through the defect states in the Si spacer layer is a key role of the interlayer exchange coupling between the top and bottom Fe layers in both the dark and photo-irradiation conditions. By comparing with the tunneling theory for the interlayer exchange coupling, which involves direct non-spin-flip tunneling, assisted non-spin-flip tunneling, and assisted spin-flip tunneling, proposed by Xiao and Li,²⁶ we see that the experimental interlayer exchange coupling behavior of the Fe/Si/Fe trilayer structure is similar to that in the theoretical model calculation (see Fig. 3 in Ref. 26). In their model, the localized defect states, the localization length of the states, and the potential barrier height of an amorphous semiconducting spacer layer were also taken into

account. The model calculation predicted that the interlayer exchange coupling strongly depended on the spacer thickness, and the ferromagnetic coupling decreases with increasing the spin-flip tunneling process. The decrease of ferromagnetic coupling was remarkable in the thin spacer thickness below 1.5 nm . The net interlayer exchange coupling was determined by the competition between the non-spin-flip tunneling and spin-flip tunneling. In addition, when the spin-flip tunneling process is sufficiently strong, the interlayer exchange coupling shows the oscillatory exchange interaction between two ferromagnetic layers. The experimental interlayer exchange coupling of Fe/Si/Fe at RT in the dark condition always showed the ferromagnetic coupling and the coupling weakened in the photo-irradiation condition for the spacer thickness to be thinner than 2.7 nm . This phenomenon is consistent with the theoretical model calculation when the electrons and holes are created by photo-irradiation in the Si spacer, because the spin-flip tunneling process increases with the concentration of the localized electrons and holes. Furthermore, the laser power dependence of magnetization reversal in Fig. 4 supports the above-mentioned interpretation. Thus we can conclude that the behavior of the interlayer exchange coupling in the Fe/Si/Fe trilayer structure at RT is qualitatively understood by the assisted tunneling theory with spin-flip process in the semiconducting spacer layer.

IV. SUMMARY

We have prepared the Fe(3 nm)/Si(0.5–6.0 nm)/Fe(10 nm) trilayer structure by e-beam evaporators at RT. The magnetization reversal process of the Fe/Si/Fe trilayer structure was measured in remanent states using SP-SEM under dark and photo-irradiation conditions. The dependence of the interlayer exchange coupling on the nominal Si spacer thickness was obtained from the magnetization reversal process. We found that the interlayer exchange coupling is always ferromagnetic for the Fe/Si/Fe trilayer structure in the entire range of the nominal Si spacer thickness in both the dark and photo-irradiation conditions. By the photo-irradiation, we found that the interlayer exchange coupling is modified in the nominal Si spacer thickness below 2.7 nm even though it is at RT. These behaviors can be qualitatively understood by the assisted tunneling theory with spin-flip processes.

ACKNOWLEDGMENTS

The authors would like to acknowledge valuable advice from Professor J. Nishizawa. This work was performed at RIKEN Photodynamics Research Center.

*On leave from RIKEN Photodynamics Research Center.

¹P. Grunberg, R. Schreiber, Y. Pang, M. B. Brodsky, and H. Sowers, *Phys. Rev. Lett.* **57**, 2442 (1986).

²M. N. Baibich, J. M. Broto, A. Fert, F. Nguyen Van Dau, F. Petroff, P. Etienne, G. Creuzet, A. Friederich, and J. Chazelas, *Phys. Rev. Lett.* **61**, 2472 (1988).

³S. S. P. Parkin, R. Bhadra, and K. P. Roche, *Phys. Rev. Lett.* **66**, 2152 (1991).

⁴K. O'Grady, S. J. Greves, and S. M. Thompson, *J. Magn. Magn. Mater.* **156**, 253 (1996).

⁵J. Unguris, R. J. Celotta, and D. T. Pierce, *Phys. Rev. Lett.* **79**, 2734 (1997).

⁶T. Mewes, B. F. P. Roos, S. O. Demokritov, and B. Hillebrands, *J. Appl. Phys.* **87**, 5064 (2000).

⁷R. Gupta, M. Weisheit, H.-U. Krebs, and P. Schaaf, *Phys. Rev. B* **67**, 075402 (2003).

- ⁸S. Toscano, B. Briner, H. Hopster, and M. Landolt, *J. Magn. Magn. Mater.* **114**, L6 (1992).
- ⁹B. Briner and M. Landolt, *Phys. Rev. Lett.* **73**, 340 (1994).
- ¹⁰J. E. Mattson, S. Kumar, E. E. Fullerton, S. R. Lee, C. H. Sowers, M. Grimsditch, S. D. Bader, and F. T. Parker, *Phys. Rev. Lett.* **71**, 185 (1993).
- ¹¹M. Anas, C. Bellouard, and M. Vergnat, *J. Appl. Phys.* **96**, 1159 (2004).
- ¹²C. Martinez Boubeta, J. M. de Teresa, J. L. Costa-Kramer, J. Anguita, D. Serrate, J. I. Arnaudás, M. R. Ibarra, A. Cebollada, and F. Briones, *J. Appl. Phys.* **94**, 4006 (2003).
- ¹³K. Inomata, K. Yusu, and Y. Saito, *Phys. Rev. Lett.* **74**, 1863 (1995).
- ¹⁴P. Walser, M. Schleberger, P. Fuchs, and M. Landolt, *Phys. Rev. Lett.* **80**, 2217 (1998).
- ¹⁵P. Walser, M. Hunziker, T. Speck, and M. Landolt, *Phys. Rev. B* **60**, 4082 (1999).
- ¹⁶Y. Iwasaki, K. Bessho, J. Kondis, H. Ohmori, and H. Hopster, *Appl. Surf. Sci.* **113-114**, 155 (1997).
- ¹⁷S. Ueda, Y. Iwasaki, Y. Uehara, and S. Ushioda, *Jpn. J. Appl. Phys.* **45**, 5004 (2006).
- ¹⁸Y. Saito, K. Inomata, and K. Yusu, *J. Appl. Phys.* **35**, L100 (1996).
- ¹⁹J. Kohlhepp, M. Valkier, A. van der Graaf, and F. J. A. den Broeder, *Phys. Rev. B* **55**, R696 (1997).
- ²⁰J. J. de Vries, J. Kohlhepp, F. J. A. den Broeder, R. Coehoorn, R. Jungblut, A. Reinders, and W. J. M. de Jonge, *Phys. Rev. Lett.* **78**, 3023 (1997).
- ²¹R. R. Gareev, D. E. Burgler, M. Buchmeier, D. Olligs, R. Schreiber, and P. Grunberg, *Phys. Rev. Lett.* **87**, 157202 (2001).
- ²²R. Klasges, C. Carbone, W. Eberhardt, C. Pampuch, O. Rader, T. Kachel, and W. Gudat, *Phys. Rev. B* **56**, 10801 (1997).
- ²³P. Bruno and C. Chappert, *Phys. Rev. Lett.* **67**, 1602 (1991).
- ²⁴Z. P. Shi and B. M. Klein, *J. Appl. Phys.* **79**, 4776 (1996).
- ²⁵See, e.g., N. F. Mott and E. A. Davis, *Electronic Processes in Non-Crystalline Materials*, 2nd ed. (Clarendon, Oxford, 1979).
- ²⁶M. W. Xiao and Z. Z. Li, *Phys. Rev. B* **54**, 3322 (1996).